THIRD EDITION

HANDBOOK OF

PROTEOLYTIC

ENZYMES

VOLUME 1

EDITED BY

NEIL D. RAWLINGS & GUY S. SALVESEN

Catalytic Pathways of Aspartic Peptidases

Introduction

The history of the carboxyl peptidases, initially encompassing only the enzymes containing catalytic aspartates, is a long one with many fascinating turns of event. This history has been told beautifully in a review by Fruton [1], whereas a review of the historical aspects of the structural results on aspartic peptidases has been presented by Blundell *et al*. [2].

The early mechanistic history of aspartic peptidases was fraught with problems revolving around the question of whether or not the intermediates on the hydrolytic pathway were covalently attached to the enzyme [3,4]. It was Fruton who first suggested that the intermediate in the hydrolytic reaction may not be covalently attached to pepsin as an acyl nor as an amino enzyme [5]. Subsequent work on the structural aspects of several aspartic peptidases confirmed that access to the two active

site aspartate residues from which this family of peptidases derives its name (Asp32 and Asp215 in pepsin numbering that will be used consistently in this chapter, rather than the numbers from the original publications), was very restricted due to the limited solvent accessibility of these residues [6,7].

Aspartic peptidases are either cellular, pepsin-like enzymes (clan AA, family A1), or homodimeric enzymes originally identified in retroviruses (retropepsins, clan AA, family A2), but later discovered also in higher organisms. Enzymatic properties of these peptidases will be discussed here in greatest detail. Some other enzymes were also considered at one time to be aspartic peptidases and were historically listed together with pepsins, but were later shown to have unique catalytic mechanisms that utilize the side chains of glutamic acid and glutamine. Enzymatic mechanisms of the latter family of enzymes will also be discussed in this chapter, albeit briefly.

Enzymatic Mechanism of Aspartic Peptidases

The substrate binding cleft of the cellular aspartic peptidases extends for 7 or 8 amino acid residues (approximately from P5 to P3′ − Figure 2.1) and is formed where the N-terminal domain and the C-terminal domain meet. Centrally located in this cleft are the two aspartic acid residues, each surrounded by virtually identical supporting motifs that are related by an approximate 2-fold axis running between the carboxyl groups of the two aspartates. The two aspartates (32 and 215) are commonly found in the Asp-Thr/Ser-Gly-Thr/Ser motif that is important for establishing and maintaining the proper environment for the carboxyl groups. The clefts in retropepsins are slightly shorter, usually accommodating only residues from P3 to P3′ [8].

A schematic diagram of the most important active site residues in pepsins is shown in Figure 2.2A, whereas the corresponding hydrogen bonding interactions in selected uninhibited forms of pepsins and retropepsins are summarized in Table 2.1. The carboxyl groups of the two aspartate residues are approximately co-planar and the water molecule that is bound between them lies in the common plane. In spite of the different resolution of the several determinations and the differences in the pH of the crystals, the distances are sufficiently similar for common bonds to be averaged. The distance between the two inner oxygen atoms of the aspartates (A) is greater than or equal to the sum of their van der Waals radii (2×1.4 Å). This does not necessarily imply the presence of a hydrogen bond between the two aspartates. Distances B and C are approximately equal suggesting that one of the protons on the water molecule sits midway between the two
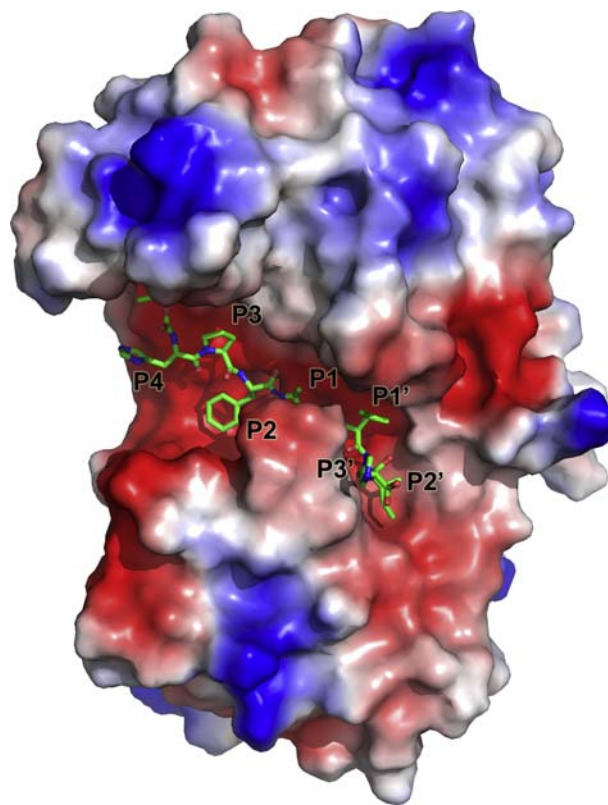
FIGURE 2.1   A view of the substrate binding cleft in endothiapepsin based on the atomic resolution crystal structure of a complex with the hydroxyethylene-containing inhibitor H261 (PDB code 1OEX − [38]). The surface of the enzyme is rendered and colored according to charge, whereas H261 (Boc-His-Pro-Phe-Ala-Lov-Ile-His) bound at the active site is shown as a ball-and-stick model. The residues from the flap make intimate contact with the P1 residue of the substrate (or the inhibitor). Hydrogen bonding and van der Waals interactions position the scissile peptide appropriately for nucleophilic attack by the general-base activated water molecule. Atomic color coding for the inhibitor: green, carbon; blue, nitrogen; red, oxygen.

oxygen atoms in a bifurcated hydrogen bond. Distances D and E differ by 0.45 Å and are consistent with a proton on the outer oxygen of Asp32 and a hydrogen bond from the second water proton to the inner oxygen of Asp32 (O...O distance = 2.76 Å).

The simplest interpretation of these hydrogen-bonding distances is shown in Figure 2.2B. In this interpretation of the active site of the enzyme in the ground state, Asp215 would be negatively charged and Asp32 would be a neutral carboxylic acid. The active center of aspartic peptidases has two pK_a values, one of ∼1.5 and the other ∼4.5. The proton distribution shown in Figure 2.2B is consistent with established, experimental observations [4,9,10]. However, the requirement that the aspartates and the catalytic water be coplanar was recently questioned on the basis of a re-refined structure of plasmepsin II [11] in which considerable deviation from planarity was noticed. A suggestion was made that the planarity is

enforced by the cryogenic temperature of data collection but not necessarily present under biologically relevant conditions. That argument, however, is counteracted by the many structures of aspartic peptidases solved at room temperature, including some at very high resolution and/or solved using neutrons rather than X-rays [12,13].
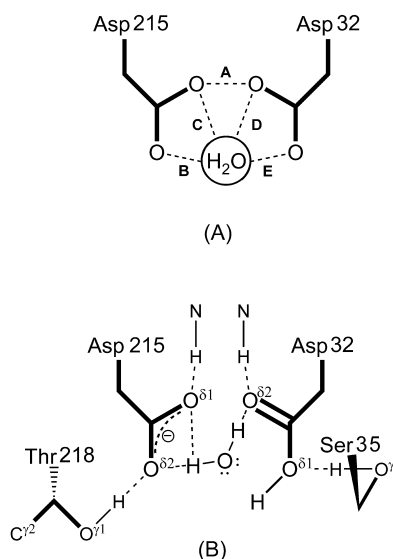
The enzymatic mechanism is most fully characterized for serine peptidases, thus providing a point of comparison with the mechanism of pepsins. A large number of structures of the serine peptidases show the detailed interactions of enzyme-substrate complexes [14]. These structures are protein inhibitors (*e.g.* turkey ovomucoid third domain [OMTKY3] [15] complexed to a variety of serine peptidases, *e.g.* α-chymotrypsin [16], *Streptomyces griseus* peptidase B (SGPB) [17], etc. Although the protein inhibitors are excellent inhibitors of the serine peptidases, they are also poor substrates. The enzyme-protein inhibitor complexes are therefore reasonable mimics of enzyme-substrate complexes expected for peptide hydrolysis catalyzed by serine peptidases.

Comparisons of the serine peptidase-protein inhibitor complexes (α-chymotrypsin -OMTKY3) with the tetrahedral intermediate mimics of the aspartic peptidase hydrolytic reaction are very revealing (Figure 2.3). Figure 2.3A shows the structure of the Iva-Val-Val-difluorostatone methylester inhibitor bound in the active site of penicillopepsin alone [18]; Figure 2.3B is a superposition of this structure and OMTKY3 bound in the active site of α-chymotrypsin. A comparison of these views shows that the formation of the tetrahedral intermediate in both the serine peptidases and the

FIGURE 2.2 Schematic diagrams of the active sites of aspartic peptidases. (A) Catalytic aspartates and the putative hydrogen bonds with the catalytic water molecule. (B) Distribution of charges and hydrogen bonds to the residues interacting with the catalytic aspartates.

TABLE 2.1 Interatomic distances in the active sites of selected pepsin-like aspartic proteases and retropepsins. Only apoenzyme structures were used in the comparisons. Since the two catalytic aspartates should be symmetric in the structures of uninhibited retropepsins, the orientation in which distance E was longer than B was arbitrarily selected

Pepsins	PDB	Resol.Å	A	B	C	D	E
Endothiapepsin	1OEW	0.9	2.93	2.92	2.96	2.76	3.13
Rhizopuspepsin pH 4.6	1UH7	2.1	2.86	2.71	2.89	2.78	3.14
Rhizopuspepsin pH 6.0	2APR	1.8	3.11	2.92	2.83	2.81	3.37
Rhizopuspepsin pH 7.0	1UH9	2.0	2.99	2.90	2.83	2.78	3.22
Rhizopuspepsin pH 8.0	1UH8	2.3	3.07	2.84	2.79	2.77	3.24
Penicillopepsin	3APP	1.8	2.88	2.86	2.83	2.62	3.15
Human pepsin	1PSN	2.2	3.00	2.96	3.15	2.97	3.38
Porcine pepsin	4PEP	1.8	2.76	3.02	2.91	2.62	3.04
Average			2.95	2.89	2.90	2.76	3.21
Retropepsins							
RSV PR	2RSP	2.0	2.81	2.56	2.69	2.58	3.18
XMRV PR	3NR6	2.0	3.07	3.11	2.73	2.62	3.23
HIV PR (subtype A)	3IXO	1.7	3.07	2.67	3.33	3.73	3.59
Average			2.98	2.78	2.92	2.98	3.33

ΔE-D∼0.45 Å for pepsins, 0.35 Å for retropepsins

(A)

(B)
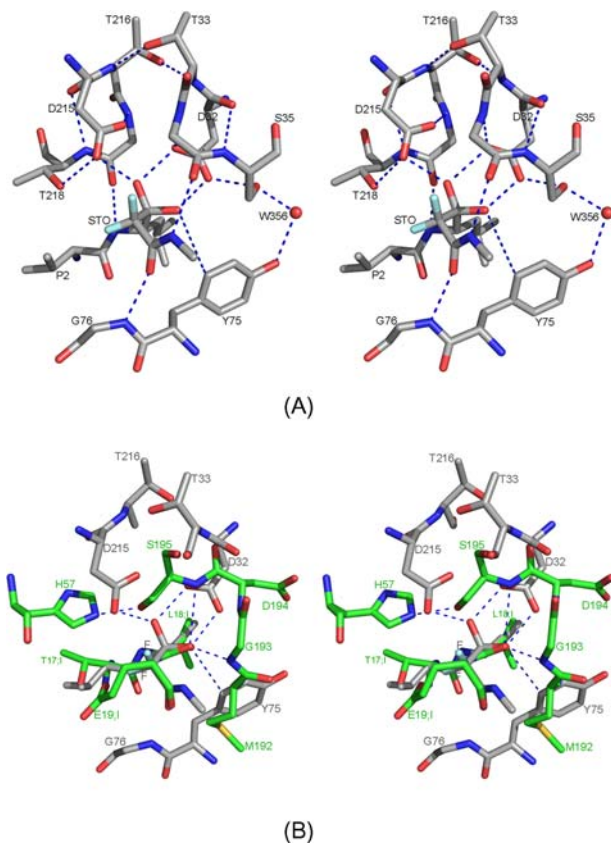
FIGURE 2.3 (A) Active site of penicillopepsin with the bound, hydrated difluorostatone inhibitor [18]. Hydrogen bonds are represented by thin dotted lines. The hydrated carbonyl forms hydrogen bonds to both oxygen atoms of the carboxylate of Asp32 as a *gem* diol. The hydrogen-bonded interactions between the hydrated difluorostatone and the two carboxyl groups of the active site (Asp32 and Asp215) are virtually identical to those expected for the tetrahedral intermediate (Figure 2.4B). (B) Superposition of aspartic peptidases and the serine peptidases. The molecular structures that are superimposed are the difluorostatone inhibitor of penicillopepsin (1APV) and the wild-type OMTKY3 complexed to α-chymotrypsin (1CHO). The following groups or atoms of the inhibitors were used in the superposition. For 1APV: Cα, C, O of Val in P2; N, Cα, Cβ, Cγ, Cδ1, Cδ2, C and O of statone in P1; C of the CF2 group. For 1CHO: Cα, C, O of Thr17I in P2; N, Cα, Cβ, Cγ, Cδ1, Cδ2, C and the carbonyl O of Leu18I in P1; N of the Glu19I of the scissile peptide. The *rms* difference for these 12 atoms is 0.21 Å. The superposition clearly shows the atomic movements necessary to form the tetrahedral intermediates in both pathways. For the serine peptidases the Ser195 Oγ moves ∼0.7 Å towards the carbonyl-carbon atom of the scissile peptide and the carbonyl carbon atom moves ∼0.5 Å towards the Ser195 Oγ as it forms a tetrahedral sp3 atom. In the aspartic peptidase mechanism, a similar movement of the carbonyl carbon of the scissile peptide occurs as it becomes pyramidal sp3 and ready to accept the nucleophilic OH−. The backbone carbon atoms of the active site region of penicillopepsin (1APV) are green and those of the OMTKY3 complex with α-chymotrypsin (1CHO) are gray. Hydrogen bonds are represented by thin dotted lines.

aspartic peptidases results from nucleophilic attack on the carbonyl carbon of the scissile peptide from the *re* face of the peptide [19]. The nucleophile of the aspartic peptidases is the water molecule bound between the two carboxyl groups (Figure 2.2) and activated to an hydroxide ion by the general base carboxylate of Asp215. In the serine peptidases the nucleophile is the Oγ of Ser195 and the general base is the imidazole of His57.

The electrophilic component assisting in the nucleophilic attack of Ser195 Oγ is the oxyanion hole. This feature in the serine peptidases is made up of two backbone NH groups (of Ser195 and Gly193) that form strong hydrogen bonds to the carbonyl oxygen atom of the P1 residue in the scissile bond. This interaction enhances the polarization of the carbonyl group and increases the electropositive character of the carbonyl-carbon atom thereby assisting in the proton transfer from Ser195 Oγ to His57 Nε2 by reducing the pK_a of Ser195. The analogous feature in the aspartic peptidases is comprised of two components: (1) the protonated carboxyl group of Asp32 that forms a hydrogen-bonded interaction with the carbonyl oxygen atom of the substrate in the E-S complex; and (2) an electrostatic interaction of the edge of the phenol ring from Tyr75 with the carbonyl oxygen of the substrate [18,20]. This latter interaction is speculative, but support for a catalytic function for Tyr75 comes from mutagenesis experiments with *Rhizomucor pusillus* pepsin in which it was replaced by 17 other amino acids and the catalytic activity of these variants assessed [21]. The only active tyrosine replacements were Phe75 (weak activity) and Asn75 (enhanced activity − k_{cat}/K_m 5.6 times higher than that of Tyr75). Presumably the side chain amide of Asn75 forms a hydrogen bond with the scissile peptide carbonyl oxygen, thereby enhancing the polarization of the carbonyl bond and the electrophilicity of the carbonyl carbon atom of the scissile peptide.

Following the nucleophilic attack on the *re* face of the scissile peptide by the general-base activated water molecule (OH−), the resulting tetrahedral intermediate adopts a *gem*-diol hydrogen-bonded interaction with the now negatively-charged carboxylate of Asp32 (Figure 2.4B). Independently determined crystal structures of penicillopepsin [18] and of endothiapepsin [22] complexed with hydrated difluoroketones confirm the possibility of such a *gem*-diol association for the tetrahedral intermediate.

At this stage in the mechanism cleavage of the peptide bond requires protonation of the leaving group nitrogen atom. Reference to the chemical hydrolytic pathway in Figure 2.4B shows that application of the stereoelectronic effect results in the lone pair electrons on the nitrogen of the scissile bond pointing away from Asp215. In order for proton transfer to take place the lone pair on the nitrogen should point towards the protonated carboxyl group of Asp215. This can take place by inversion of the absolute configuration of the nitrogen atom, a process that is extremely rapid [23].
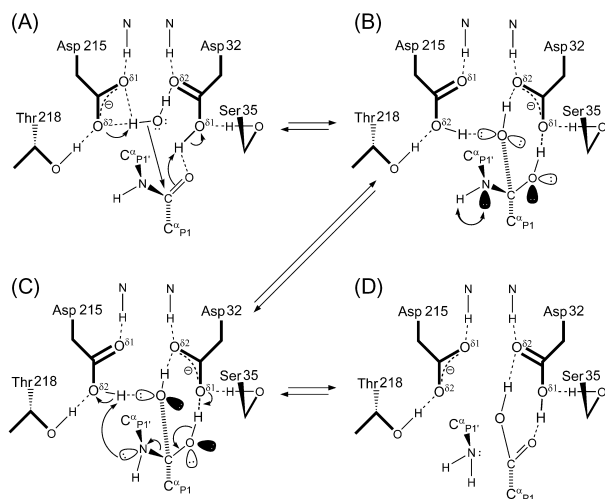
FIGURE 2.4 (A) Stylized representation of the enzyme-substrate complex. The substrate approaches the active site with the P1 side chain in the S1 binding pocket. Such models were determined from a large number of crystal structures of aspartic peptidases complexed to transition-state peptidomimetics. For the present discussion, an accurate model of an E-S complex of an aspartic peptidase has been deduced on the basis of superimposing the tetrahedral transition state mimics with the complexes of the serine peptidases with protein inhibitors such as OMTKY3 (Figure 2.3B). The nucleophilic water of the aspartic peptidases is positioned appropriately for attack on the carbonyl-carbon atom of the scissile peptide. General base assistance is achieved via the ionized carboxylate of Asp215; electrophilic assistance comes from a short hydrogen bond (LBHB) from the protonated carboxyl of Asp32. In this mechanism the proton is transferred from Asp32 to the carbonyl-oxygen atom of the scissile peptide. It could, however, be an LBHB and reside midway between the two oxygen atoms. (B) Tetrahedral intermediate. The hydroxyl attack on the carbonyl-carbon atom is assisted by the stereoelectronic effect [39] in that lone pair electrons on the carbonyl oxygen atom and on the nitrogen atom of the scissile peptide are arranged antiperiplanar to the direction of hydroxide ion attack (black lone-pair orbitals). The carboxylate of Asp32 receives hydrogen bonds from the *gem* diol of the tetrahedral intermediate. The tetrahedral intermediate is also stabilized by the proximity of the positive edge of the phenol ring of Tyr75 (not shown here). (C) Model for protonation of leaving group. In order for the peptide bond to break, the nitrogen of the scissile bond (now a tetrahedral sp^3 nitrogen atom) must be protonated to make a good leaving group ($-NH_2$). In order to facilitate the protonation from Asp215 the nitrogen atom must invert its configuration from that in (B) to place the lone-pair orbital appropriately to receive the proton. Cleavage of the peptide is also enabled by the antiperiplanar lone pair electrons (black orbitals) on each of the oxygens in the *gem* diol. (D) The bond cleavage. The proton transfer from the outer oxygen atom of the *gem* diol to Asp32 carboxylate (general base in this second case) results in the peptide bond cleavage to release a new free amino group (R′-NH₂) and a new free carboxyl group (R-COOH). Dissociation of these groups and reassociation of the active site carboxyl groups with a water molecule regenerates the active form of the enzyme (Figure 2.1B).

Transfer of the proton of the leaving group nitrogen (Figure 2.4C) is coupled to the regeneration of the protonated state of the carboxyl of Asp32. It is also coupled to cleavage of the peptide bond in a concerted

fashion. Thus, the protonated carbonyl oxygen transfers the proton to the carboxylate of Asp32. The carbonyl of the newly formed carboxyl results in addition to the peptide NH–C=O cleavage that would result on protonation of the nitrogen.

Several crystal structures of transition state intermediates (*i.e.* phosphonates) bound to penicillopepsin and endothiapepsin contain low barrier hydrogen bonds (LBHB) between the outer carboxyl oxygen of Asp32 and the phosphonate oxygen atom [13,24−26]. This bond is short (2.42−2.54 Å) and would qualify for a high energy LBHB. Release of the energy of this LBHB would assist in the peptide bond cleavage by lowering the activation energy barrier of the reaction and would return the enzymes active site to the native state. It is likely that an equivalent low barrier hydrogen bond between the analogous oxygen atoms is present in the transition state on the hydrolytic pathway of a good substrate. Such a bond would have a strong effect on the two proton transfers required during the bond cleavage reaction (Figure 2.3C, D). As the proton of the LBHB becomes associated more with Asp32, the energy would be used to facilitate the proton transfer from Asp215 to the leaving group nitrogen as well as lowering the activation energy barrier for peptide bond cleavage. It is imperative that the LBHB occurs in the transition state as it does in this mechanism and as suggested by Cleland [27].

The LBHB mentioned above is different from the putative LBHB between the carboxyl groups of Asp32 and Asp215, previously invoked to explain the kinetic mechanism of aspartic peptidases [28]. That argument hinged on a ten atom hydrogen-bonded cyclic structure for the water molecule and the two carboxyl groups of the active site (see Figure 2.5) and was principally based on *ab initio* molecular dynamic simulations on HIV-1 protease [29]. An LBHB between the two catalytic aspartates would require the distance between their inner oxygens to be shorter than 2.5 Å [27]. As shown in Table 2.1, there is no case in which such distance (A) is shorter than 2.76 Å (average 2.95 Å), thus it represents a normal oxygen-oxygen contact. In addition, for the LBHB to be effective in lowering the activation
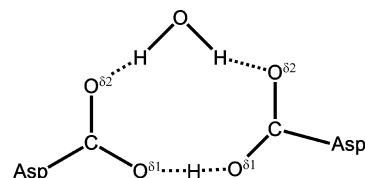
FIGURE 2.5 A proposed configuration of the two aspartic acid residues and the bound water in the HIV peptidase structure as deduced from *ab initio* molecular dynamics simulations [29]. There is no evidence for the low barrier hydrogen bond between the carboxyl groups from any of the X-ray or neutron crystallographic studies done on aspartic peptidases or their inhibitor complexes (see Table 2.1).

energy barrier of the reaction being catalyzed, it should not occur in the ground state but rather should be formed in a transition state or in a transient intermediate. However, none of the structures of transition-state mimics, *i.e.* the hydrated difluorostatone [18] discussed here or the phosphonate inhibitors of penicillopepsin [24−26] have a short distance between the inner carboxylate oxygens of the catalytic aspartates.

Finally, atomic resolution X-ray and medium resolution neutron diffraction studies of endothiapepsin complexed with a transition state analog inhibitor, PD-135,040, has determined with reasonable certainty the protonation states of the active site groups [13]. Asp32 is best interpreted as ionized, *i.e.* negatively charged, and Asp215 is protonated. This charge distribution corresponds exactly with that of the chemical mechanism deduced from the many crystallographic structures and depicted in Figure 2.4B,C. The neutron structure determination has no evidence of a proton between the inner oxygen atoms of Asp32 and Asp215. The distance between these atoms is 2.93 Å, again confirming that there is no LBHB between the active site aspartate residues.

The mechanism of retropepsins follows most likely the mechanism described above for the pepsin-like enzymes. The main difference is that there cannot be any distinction between the two aspartates (Asp25 in the enzyme from the human immunodeficiency virus) in the native enzyme, since it is a symmetric homodimer. However, the symmetry is broken as soon as a substrate is bound, allowing one of the aspartates to assume the function of Asp32, and the other of Asp215. Structural data for the complexes of retropepsins with inhibitors support this assumption, and indeed the mechanism employed by this family of peptidases was discussed in some detail in the past [30].

Histo-aspartic protease from *Plasmodium falciparum* presents an unusual variant of aspartic peptidases. Despite the fold being similar to other pepsin-like enzymes [31], Asp32 is replaced in this enzyme by histidine, and several other active site residues also differ from the consensus. Whereas the detailed mechanism of enzymatic activity of histo-aspartic protease is still not fully established, modeling and computational studies suggested that Asp215 might act as both a nucleophile and an electrophile, whereas the role of His32 would be only to assist in the reaction and increase the rate by up to four orders of magnitude [32].

On the other hand, the mechanism of peptide bond hydrolysis in the aspartic peptidase family of enzymes seems to be reasonably well established [18,33,34]. The majority of the details have been gleaned from structural studies of these enzymes with transition state mimics bound to the active sites. Although proton locations cannot be inferred with confidence from the X-ray crystal

structures, the donor−acceptor distances are consistent with the mechanism depicted in Figure 2.4. In this mechanism, the hydroxide ion is the nucleophile and its formation is assisted by the general-base function of Asp215. The tetrahedral intermediate resulting from the nucleophilic attack on the carbonyl carbon atom is stabilized by *gem* diol hydrogen bonding to Asp32. One of these hydrogen bonds is a LBHB whose energy can be used to lower the activation energy of the peptide bond cleavage reaction. The leaving group nitrogen is protonated by the general acid function of protonated Asp215.

Enzymatic Mechanism of Glutamic Peptidases

The three-dimensional structures of several enzymes known to utilize carboxyl-bearing residues in their catalytic mechanism, yet not being inhibited by pepstatin A, have shown that their overall structures and the catalytic centers were not related to those of pepsins. This new family of carboxyl peptidases, now designated clan GA, family G1, was identified in 2004, with the founding members being scytalidocarboxyl peptidase B (SCP-B) from *Scytalidium lignicolum* ATCC24568 [35] and aspergilloglutamic peptidase from *Aspergillus niger* [36]. On the basis of the conserved catalytic residues in the active site (a glutamic acid and glutamine), the name given to the enzyme family was eqolisin.

Unlike the pepsins, eqolisin molecules consist of a β-sandwich, with the catalytic residues residing on two non-adjacent strands (Figure 2.6A). A catalytic mechanism
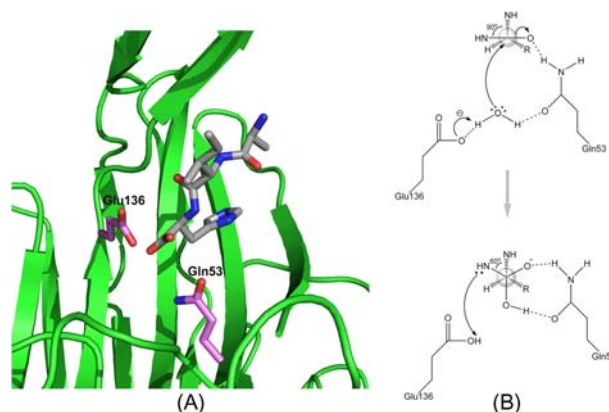
FIGURE 2.6 Structure and mechanism of eqolisins. (A) A close-up of the secondary structure of SCP-B showing the location of the active site residues, Glu136 and Gln53. Subsites P3 to P1 of the substrate-binding site are delineated by the bound product tripeptide Ala-Ile-His that resulted from hydrolysis of angiotensin II by SCP-B. (B) The proposed catalytic mechanism of SCP-B. The water molecule hydrogen-bonded to both Glu136 and Gln53 is the nucleophile. The general base is the carboxylate of Glu136. The side-chain amide of Gln53 assists in the nucleophilic attack and stabilizes the tetrahedral intermediate by hydrogen bonding.

for this family was first proposed by Fujinaga *et al.* [35] on the basis of the structures of native SCP-B and its complex with hydrolytic products of angiotensin II (Asp-Arg-Val-Tyr-Ile-His-Pro-Phe) (Figure 2.6B). A water molecule, analogous to the catalytic water in aspartic peptidases, is located within hydrogen bonded distances from the side chains of Glu136 and Gln53. In the structure of the product complex, the ligands included a tripeptide, Ala-Ile-His, occupying subsites P1-P3, and a single tyrosine. The tripeptide most likely corresponds to the sequence Tyr-Ile-His, with the side chain of Tyr disordered and thus represented as Ala. The ligand binds in an extended conformation, with the OXT atom of the P1 His carboxyl group at its C terminus forming a hydrogen bond with the side-chain carboxyl group of Glu136. A van der Waals contact is made between $O\varepsilon1$ of Gln53 and O of P1 His. The interpretation of this observation is that the side-chain carboxyl group of Glu136 is protonated and a second hydrogen bond to the P1 His OXT is donated by the $N\varepsilon2$ of Gln53. In addition, the $N\varepsilon2$ atom of the P1 His imidazolium group forms a hydrogen bond to the carboxylate of Asp57.

The structures of SCP-B can thus be used to postulate the catalytic mechanism of the eqolisins. The water molecule bound between Glu136 and Gln53 (Figure 2.6B) acts as the nucleophile that is activated to a hydroxide ion by the general base functionality of the carboxylate of Glu136. Electrophilic assistance by polarizing the carbonyl bond of the scissile peptide is provided by the side-chain amide of Gln53. The hydrogen-bonded interaction from Gln53 $N\varepsilon2$ to the substrate carbonyl oxygen is bifunctional, by assisting in the formation of the tetrahedral intermediate as well as providing stabilization of the resulting oxyanion. Gln53 provides for stabilization of the tetrahedral intermediate by donating a hydrogen bond from its $N\varepsilon2$ to the oxyanion of the tetrahedral intermediate and by receiving a hydrogen bond to $O\varepsilon1$ from the OH of the attacking water molecule. The nucleophilic attack takes place on the *si*-face of the scissile peptide. This direction of attack is seen only in the papain-like cysteine peptidase family; it is the *re*-face attack that takes place in the serine, aspartic, and metallopeptidases.

Protonation of the leaving-group nitrogen is an obligatory step in any hydrolytic mechanism for an amide. By analogy with the aspartic and metallopeptidases, it is likely that the proton donor will be the protonated Glu136. The tetrahedral character of the nitrogen atom in the intermediate will place the lone-pair electrons on the nitrogen in an appropriate position to abstract the proton from the carboxyl group of Glu136.

Another family of glutamic peptidases, G2, is represented by the C-terminal domain of gene product 12 of the tailed bacteriophage $\varphi29$ [37]. It has been postulated

that self-processing of this protein is catalyzed by Glu695 which attacks the carbonyl carbon of the substrate residue Ser691, possibly assisted by the side chain of Asp692. Mutation of either Glu695 or Asp692 prevented autoprocessing, but structural data are not detailed enough to enable full analysis of the catalytic mechanism.

It is thus clear that although the mechanisms of enzymatic activity of the aspartic and glutamic peptidases share some similarities, there are also very important differences between these enzymes which are now separated into different catalytic types.

References

[1] Fruton, J.S. (2002). A history of pepsin and related enzymes. *Q. Rev. Biol.* 77(2), 127−147.

[2] Blundell, T.L., Guruprasad, K.A.A., Williams, M., Sibanda, B.L., Dhanaraj, V. (1998). The aspartic proteinases. An historical overview. *Adv. Exp. Med. Biol.* 436, 1−13.

[3] Knowles, J.R. (1970). On the mechanism of action of pepsin. *Philos. Trans. R Soc. Lond. B Biol. Sci.* 257(813), 135−146.

[4] Clement, G.E. (1973). Catalytic activity of pepsin, in: *Progress in Bioorganic Chemistry*, Kaiser, E.T., Kezdy, F.J., eds., New York: John Wiley & Sons, pp. 177−238.

[5] Fruton, J.S. (1976). The mechanism of the catalytic action of pepsin and related acid proteinases. *Adv. Enzymol. Relat. Areas Mol. Biol.* 44, 1−36.

[6] Hsu, I.N., Delbaere, L.T., James, M.N., Hofmann, T. (1977). Penicillopepsin from *Penicillium janthinellum* crystal structure at 2.8 Å and sequence homology with porcine pepsin. *Nature* 266 (5598), 140−145.

[7] James, M.N., Hsu, I.N., Delbaere, L.T. (1977). Mechanism of acid protease catalysis based on the crystal structure of penicillopepsin. *Nature* 267(5614), 808−813.

[8] Wlodawer, A., Erickson, J.W. (1993). Structure-based inhibitors of HIV-1 protease. *Annu. Rev. Biochem.* 62, 543−585.

[9] Cornish-Bowden, A.J., Knowles, J.R. (1969). The pH-dependence of pepsin-catalysed reactions. *Biochem. J.* 113(2), 353−362.

[10] Clement, G.E., Rooney, J., Zakheim, D., Eastman, J. (1970). The pH dependence of the dephosphorylated pepsin-catalyzed hydrolysis of *N*-acetyl-L-phenylalanyl-L-tyrosine methyl ester. *J. Am. Chem. Soc.* 92(1), 186−189.

[11] Robbins, A.H., Dunn, B.M., Agbandje-McKenna, M., McKenna, R. (2009). Crystallographic evidence for noncoplanar catalytic aspartic acids in plasmepsin II resides in the Protein Data Bank. *Acta. Crystallogr.* D65(Pt 3), 294−296.

[12] Coates, L., Erskine, P.T., Wood, S.P., Myles, D.A., Cooper, J.B. (2001). A neutron Laue diffraction study of endothiapepsin: implications for the aspartic proteinase mechanism. *Biochemistry* 40(44), 13149−13157.

[13] Coates, L., Tuan, H.F., Tomanicek, S., Kovalevsky, A., Mustyakimov, M., Erskine, P., Cooper, J. (2008). The catalytic mechanism of an aspartic proteinase explored with neutron and X-ray diffraction. *J. Am. Chem. Soc.* 130(23), 7235−7237.

[14] Bode, W., Huber, R. (1992). Natural protein proteinase inhibitors and their interaction with proteinases. *Eur. J. Biochem.* 204(2), 433−451.

[15] Laskowski, M., Qasim, M.A. (2000). What can the structures of enzyme-inhibitor complexes tell us about the structures of enzyme substrate complexes? *Biochim. Biophys. Acta.* 1477(1-2), 324−337.

[16] Fujinaga, M., Sielecki, A.R., Read, R.J., Ardelt, W., Laskowski, M. Jr., James, M.N. (1987). Crystal and molecular structures of the complex of alpha-chymotrypsin with its inhibitor turkey ovomucoid third domain at 1.8 Å resolution. *J. Mol. Biol.* 195(2), 397−418.

[17] Read, R.J., Fujinaga, M., Sielecki, A.R., James, M.N. (1983). Structure of the complex of Streptomyces griseus protease B and the third domain of the turkey ovomucoid inhibitor at 1.8-Å resolution. *Biochemistry* 22(19), 4420−4433.

[18] James, M.N., Sielecki, A.R., Hayakawa, K., Gelb, M.H. (1992). Crystallographic analysis of transition state mimics bound to penicillopepsin: difluorostatine- and difluorostatone-containing peptides. *Biochemistry* 31(15), 3872−3886.

[19] James, M.N.G. (1994). Convergence of active-centre geometries among the proteolytic enzymes, in: *Proteolysis and Protein Turnover*, Bond, J.S., Barrett, A.J., eds., Brookfield, Vermont: Portland Press, pp. 1−8.

[20] Blundell, T.L., Cooper, J., Foundling, S.I., Jones, D.M., Atrash, B., Szelke, M. (1987). On the rational design of renin inhibitors: X-ray studies of aspartic proteinases complexed with transition-state analogues. *Biochemistry* 26(18), 5585−5590.

[21] Park, Y.N., Aikawa, J., Nishiyama, M., Horinouchi, S., Beppu, T. (1996). Involvement of a residue at position 75 in the catalytic mechanism of a fungal aspartic proteinase, *Rhizomucor pusillus* pepsin. Replacement of tyrosine 75 on the flap by asparagine enhances catalytic efficiency. *Protein Eng.* 9(10), 869−875.

[22] Veerapandian, B., Cooper, J.B., Sali, A., Blundell, T.L., Rosati, R.L., Dominy, B.W., Damon, D.B., Hoover, D.J. (1992). Direct observation by X-ray analysis of the tetrahedral 'intermediate' of aspartic proteinases. *Protein Sci.* 1(3), 322−328.

[23] Bizzozero, S.A., Dutler, H. (1981). Stereochemical aspects of peptide hydrolysis catalyzed by sereine proteases of the chymotrypsin type. *Bioorganic Chem* 10, 46−62.

[24] Fraser, M.E., Strynadka, N.C., Bartlett, P.A., Hanson, J.E., James, M.N. (1992). Crystallographic analysis of transition-state mimics bound to penicillopepsin: phosphorus-containing peptide analogues. *Biochemistry* 31(22), 5201−5214.

[25] Ding, J., Fraser, M.E., Meyer, J.H.B.P.A., James, M.N.G. (1998). Macrocyclic inhibitors of penicillopepsin. 2. X-Ray crytallographic analyses of penicillopepsin complexed with a P3-P1 macrocyclic peptidyl inhibitor and with its two acyclic analogues. *J. Am. Chem. Soc.* 120, 4610−4621.

[26] Khan, A.R., Parrish, J.C., Fraser, M.E., Smith, W.W., Bartlett, P.A., James, M.N. (1998). Lowering the entropic barrier for binding conformationally flexible inhibitors to enzymes. *Biochemistry* 37(48), 16839−16845.

[27] Cleland, W.W. (2000). Low-barrier hydrogen bonds and enzymatic catalysis. *Arch. Biochem. Biophys.* 382(1), 1−5.

[28] Northrop, D.B. (2001). Follow the protons: a low-barrier hydrogen bond unifies the mechanisms of the aspartic proteases. *Acc. Chem. Res.* 34(10), 790−797.

[29] Piana, S., Carloni, P. (2000). Conformational flexibility of the catalytic Asp dyad in HIV-1 protease: An *ab initio* study on the free enzyme. *Proteins* 39(1), 26−36.

[30] Jaskólski, M., Tomasselli, A.G., Sawyer, T.K., Staples, D.G., Heinrikson, R.L., Schneider, J., Kent, S.B., Wlodawer, A. (1991). Structure at 2.5 Å resolution of chemically synthesized human immunodeficiency virus type 1 protease complexed with a hydroxyethylene-based inhibitor. *Biochemistry* 30, 1600−1609.

[31] Bhaumik, P., Xiao, H., Parr, C.L., Kiso, Y., Gustchina, A., Yada, R.Y., Wlodawer, A. (2009). Crystal structures of the histo-aspartic protease (HAP) from *Plasmodium falciparum. J. Mol. Biol.* 388(3), 520−540.

[32] Bjelic, S., Aqvist, J. (2004). Computational prediction of structure, substrate binding mode, mechanism, and rate for a malaria protease with a novel type of active site. *Biochemistry* 43(46), 14521−14528.

[33] Suguna, K., Padlan, E.A., Smith, C.W., Carlson, W.D., Davies, D.R. (1987). Binding of a reduced peptide inhibitor to the aspartic proteinase from *Rhizopus chinensis*: Implications for a mechanism of action. *Proc. Natl. Acad. Sci. USA* 84, 7009−7013.

[34] Davies, D.R. (1990). The structure and function of the aspartic proteinases. *Annu. Rev. Biophys. Biophys. Chem.* 19, 189−215.

[35] Fujinaga, M., Cherney, M.M., Oyama, H., Oda, K., James, M.N. (2004). The molecular structure and catalytic mechanism of a novel carboxyl peptidase from *Scytalidium lignicolum. Proc. Natl. Acad. Sci. USA* 101(10), 3364−3369.

[36] Sasaki, H., Nakagawa, A., Muramatsu, T., Suganuma, M., Sawano, Y., Kojima, M., Kubota, K., Takahashi, K., Tanokura, M. (2004). The three-dimensional structure of aspergilloglutamic peptidase from *Aspergillus niger. Proc. Japan Acad.* 80, 435−438.

[37] Xiang, Y., Leiman, P.G., Li, L., Grimes, S., Anderson, D.L., Rossmann, M.G. (2009). Crystallographic insights into the autocatalytic assembly mechanism of a bacteriophage tail spike. *Mol. Cell* 34(3), 375−386.

[38] Erskine, P.T., Coates, L., Mall, S., Gill, R.S., Wood, S.P., Myles, D.A., Cooper, J.B. (2003). Atomic resolution analysis of the catalytic site of an aspartic proteinase and an unexpected mode of binding by short peptides. *Protein Sci.* 12(8), 1741−1749.

[39] Deslongchamps, P. (1975). Stereoelectronic control in cleavage of tetrahedral intermediates in dydrolysis of esters and amides. *Tetrahedron* 31, 2463−2490.

Alexander Wlodawer

Macromolecular Crystallography Laboratory, National Cancer Institute-Frederick, Maryland 21702, USA. Email: wlodawer@nih.gov

Alla Gustchina

Macromolecular Crystallography Laboratory, National Cancer Institute-Frederick, Maryland 21702, USA. Email: gustchia@mail.nih.gov

Michael N.G. James

Department of Biochemistry, University of Alberta, Edmonton, Alberta T6G 2H7, Canada. Email: michael.james@ualberta.ca